ACS APPLIED MATERIALS & INTERFACES

RESEARCH ARTICLE

www.acsami.org

Realizing Visible-Light-Induced Self-Cleaning Property of Cotton through Coating N-TiO_2 Film and Loading AgI Particles

Deyong Wu*,† and Mingce Long*,‡

†School of Chemical and Environmental Engineering, Hubei University for Nationalities, Enshi, Hubei, 445000, China

‡School of Environmental Science and Engineering, Shanghai Jiao Tong University, Dong Chuan Road 800, Shanghai, 200240, China

Supporting Information

ABSTRACT: The visible-light-induced self-cleaning property of cotton has been realized by coating N-TiO_2 film and loading AgI particles simultaneously. The physical properties were characterized by means of XRD, SEM, TEM, XPS, and DRS techniques. The visible light photocatalytic activities of the materials were evaluated using the degradation of methyl orange. In comparison with TiO_2−cotton, the dramatic enhancement in the visible light photocatalytic performance of the AgI−N−TiO_2−cotton could be attributed to the synergistic effect of AgI and N−TiO_2, including generation of visible light photocatalytic activity and the effective electron−hole separations at the interfaces of the two semiconductors. The photocatalytic activity of the AgI−N−TiO_2−cotton was fully maintained upon several numbers of photodegradation cycles. In addition, according to the XRD patterns of the AgI−N−TiO_2−cotton before and after reaction, AgI was stable in the composites under visible light irradiation. Moreover, a possible mechanism for the excellent and stable photocatalytic activity of AgI−N−TiO_2−cotton under visible light irradiation was also proposed.

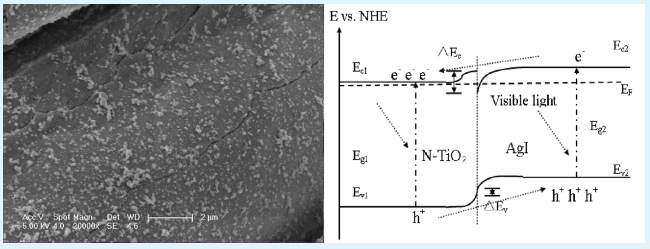

KEYWORDS: AgI, N-TiO_2, visible-light-induced, self-cleaning, low thermal resistance

INTRODUCTION

Titanium dioxide (TiO_2), as a cheap, nontoxic, highly efficient, stable, and ecologically friendly photocatalyst, has been proved to be an excellent catalyst in the degradation of organic pollutants.[1,2] However, at present, the large-scale application of TiO_2 particles as an efficient photocatalyst is limited because of the difficulty of its separation from the water treatment system. A solution is to immobilize nano-TiO_2 particles onto a suitable substrate to facilitate the practical application of the photocatalytic process. Nanosized TiO_2 particles can be immobilized on glass, activated carbon, silica materials, and polymeric materials using many different techniques.[3,4] Sol−gel processes offer an attractive means of producing TiO_2-based thin films at a low temperature, which can extend the application of TiO_2 to substrates with low thermal resistance.[5−8] Much works have been conducted on the optimization of the catalytic properties of TiO_2 films at low temperatures by using modified TiO_2 thin films.[9,10] Recently, we have successfully prepared TiO_2-coated cotton fabrics at low temperature, which possess self-cleaning properties for sterilization of bacteria and decoloration of methyl orange.[6] However, because of its wide band gap (3.2 eV for anatase), TiO_2 can only be excited under ultraviolet irradiation, which occupies only about 3−5% of the total solar irradiance at the Earth's surface. As a result, TiO_2-coated cotton fabrics only own self-cleaning property under ultraviolet irradiation.

For the sake of efficient utilization of sunlight, the self-cleaning property of cotton fabrics under visible light irradiation should be realized. Since Asahi reported the visible-light photocatalytic activity of N-doped TiO_2,[11] great effort has been made to prepare N-doped TiO_2 with the photocatalytic activity in the visible-light region.[12,13] In the present work, we described a facile and effective method to produce an aqueous N−TiO_2 nanosol at low temperature, and next prepared N−TiO_2−cotton with self-cleaning property under visible light irradiation. Meanwhile, we loaded AgI particles on the surface of N−TiO_2−cotton to improve the visible-light-induced self-cleaning property. Currently, AgI, as a visible-light photocatalyst, has attracted a great deal of interest in the field of photocatalysis. And several researchers have prepared the photocatalysts AgI/TiO_2, which are very stable under light irradiation and show high efficiency for the degradation of dyes and killing of bacteria.[14−16]

Based on above discussion, to induce an efficient visible light activity, self-cleaning AgI particles modified N−TiO_2-coated cotton fabrics (AgI−N−TiO_2−cotton) have been prepared through a sequential chemical bath deposition method. In the present work, the photocatalytic activity evaluation of the self-cleaning cotton fabrics was carried out by decomposing methyl orange under visible light irradiation and the possible origin of the highly enhanced performance was also proposed.

Received: September 15, 2011
Accepted: November 8, 2011
Published: November 08, 2011

dx.doi.org/10.1021/am201251d | ACS Appl. Mater. Interfaces 2011, 3, 4770–4774

EXPERIMENTAL SECTION

Materials. Tetrabutyl titanate ($Ti(OBu)_4$), silver nitrate ($AgNO_3$), ammonium hydroxide ($NH_3 \cdot H_2O$), potassium iodide (KI), triethylamine ($(C_2H_5)_3N$), acetylacetone ($CH_3COCH_2COCH_3$), nitric acid (HNO_3) and isopropanol (C_3H_8O) were purchased from Sinopharm Chemical Reagent Co. Ltd. All chemicals were analytical grade without further purification. Deionized water was used throughout this study.

Preparation of Anatase N-TiO_2 Hydrosol. The N−TiO_2 nanosol was prepared according to the following typical steps: under the stirring at room temperature, a mixture of 5 mL of $Ti(OBu)_4$ and 5 mL of isopropyl alcohol was added dropwise into 30 mL HNO_3 solution (0.2 mol/L). Then, the mixture was aged overnight with stirring for 12 h to obtain a transparent nanosol. Subsequently, the nanosol was treated with triethylamine for 12 h by adding 2.0 mL of TEA into the sol with stirring at ambient temperature. Then, the sol was treated under refluxing at 100 °C for 6 h. Continuous stirring is essential to keep the sol from coagulation. As control, TiO_2 nanosol was prepared in the same process but without adding TEA.

N-TiO_2 Coating Process. The cotton fabrics, which have been pretreated with the method described in our earlier study,[6] were immersed in the N−TiO_2 hydrosol for 1 min, and then pressed at a pressure of 1.25 kg cm^{-2} for 5 min. The coated substrates were heated at 60 °C in preheated oven. Finally, the fabrics were immersed in 70 °C hot water for 3 h to remove unattached N-TiO_2 particles from the fabric surface.

AgI Loading Process. Loading AgI particles on the N-TiO_2 coated fabrics was carried out by a once sequential chemical bath deposition in $[Ag(NH_3)_2]^+$ and KI aqueous solution. First, N−TiO_2−cotton fabrics were immersed in a 0.01 M $[Ag(NH_3)_2]^+$ solution for 1 h in order to adsorb large numbers of Ag^+ ions as much as possible on the surface. Second, the treated cotton fabrics were dipped into a 0.01 M KI solution for 1 h so that the absorbed Ag^+ ions on the cotton fabrics react with I^- to generate AgI particles. Lastly, the cotton fabrics were washed by a mass of water to remove unattached AgI particles from the fabric surface, and then can be used to test the properties after natural drying.

Characterization of Catalysts. X-ray powder diffraction (XRD) pattern of samples were recorded on a powder X-ray diffractometer (D/max-2200/PC, Rigaku Corporation, Japan) with Cu Ka radiation, operating at 40 kV and 30 mA, where λ = 0.15418 nm for the Cu Kα line. XPS experiments were carried out on a RBD upgraded PHI-5000C ESCA system (Perkin-Elmer, USA), the shift of the binding energy due to relative surface charging was corrected using the C 1s level at 284.6 eV as an internal standard. The structure and morphology of the coatings were investigated by the field emission scanning electron microscopy (FESEM, FEI SIRION 200, FEI, USA). The structure and the morphology of the catalyst powders were observed by Transmission Electron Microscope (TEM, JEM-100CX, JEOL, Japan). UV−vis diffuse reflectance spectra (DRS) of the samples were recorded on a UV−vis spectrophotometer (TU-1901) with an integrating sphere attachment. The analyzed range was 230−800 nm, and $BaSO_4$ was used as a reflectance standard.

Photocatalytic Degradation of MO under Visible-Light Irradiation. Methyl orange (MO) was selected as a model chemical to evaluate the activity of the catalysts. A 1000 W Xe lamp was used as the light source of a homemade photoreactor, surrounded with a water circulation facility at the outer wall through a quartz jacket. The short wavelength components (λ< 400 nm) of the light were cut off using a glass optical filter. The distance between the lamp and the center of the beaker was 100 cm. Before irradiation, 50 mL MO solution (5 mg/L) with a piece of 4 cm ×4 cm AgI−N−TiO_2−cotton was stirred in the dark for 30 min to achieve adsorption equilibrium. MO solution was taken out at regular time intervals and the residual MO concentration was monitored at 464 nm using a UV−vis spectrophotometer (UNICO 7200).

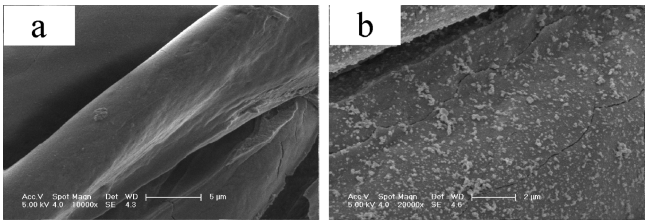

Figure 1. Typical SEM images of (a) N-TiO_2−cotton and (b) AgI−N−TiO_2−cotton.

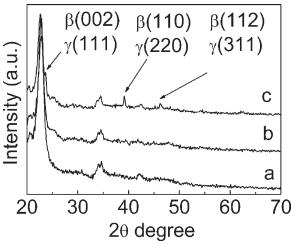

Figure 2. XRD of (a) cotton, (b) N−TiO_2−cotton, and (c) AgI−N−TiO_2−cotton.

RESULTS AND DISCUSSION

The microscope morphologies of the as-prepared N−TiO_2−cotton and AgI−N−TiO_2−cotton were investigated by SEM observation. Figure 1a shows a typical SEM image of the N−TiO_2−cotton, which displays a homogeneous N−TiO_2 coating on the surface of cotton, resulting in a smooth surface covered by N−TiO_2 nanoparticles, which are composed of polycrystalline aggregates of an anatase nanostructure (see Figure S1 in the Supporting Information). Figure 1b is a low-magnification SEM image of the AgI−N−TiO_2−cotton, whose surface has been covered with a large number of AgI particles, which shows a slight agglomeration with a size of several hundred nanometers. EDX spectrum of AgI−N−TiO_2−cotton has been measured (see Figure S2 in the Supporting Information, which reveals the existence of Ti, Ag, I, etc. The atomic content of Ti is 12.17%, but Ag is 0.55%, suggesting that the content of AgI is about 3% that of TiO_2. Moreover the EDX map also supported that the distribution of AgI particles over the cotton surface is corresponded to the dots observed from the SEM images (see Figure S3, Supporting Information. Therefore, a contact between the AgI and N−TiO_2 has been fabricated over the cotton surface.

XRD patterns of the cotton, N−TiO_2−cotton and AgI−N−TiO_2−cotton are shown in Figure 2. Because the diffraction peaks of cotton are very strong (see Figure S4 in the Supporting Information, the diffraction peaks of N-TiO_2 cannot be visibly displayed in the N−TiO_2−cotton sample. As a matter of fact, the anatase is observed for the pure N−TiO_2 nanoparticle powders (see Figure S5 in the Supporting Information), which was further confirmed by the SAED analysis (see Figure S1 in the Supporting Information). The crystalline size of N-TiO_2 can be estimated as 4.7 nm according to Scherrer's equation.[17] Comparing the diffraction profile of AgI−N−TiO_2−cotton with that of cotton and N−TiO_2−cotton, new strong diffraction peaks appear at the position about 23.6, 39.2, and 46.2°, which correspond to the peaks of (002), (110), and (112) diffraction peaks of β-AgI overlapped by the peaks of γ-AgI.[14,18] In fact, AgI always coexist

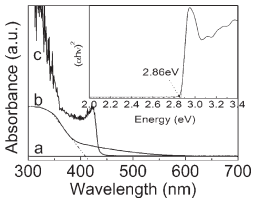

Figure 3. UV−vis diffuse reflectance spectra of (a) cotton, (b) N−TiO_2−cotton, and (c) AgI−N−TiO_2−cotton. The inset is the estimated band gap of AgI by Kubelka−Munk function.

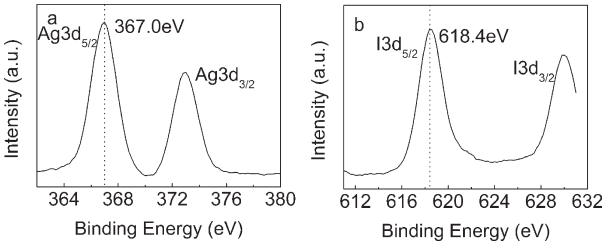

Figure 4. XPS spectra of (a) Ag3d and (b) I3d for AgI−N−TiO_2−cotton.

in a hexagonal β phase with a wurtzite structure or a cubic γ phase at ambient conditions.[19,20]

The optical absorption of the cotton, N−TiO_2−cotton, and AgI−N−TiO_2−cotton were measured using UV−vis diffuse reflectance spectra. As shown in Figure 3, pristine cotton has no ability to absorb UV and visible light, and the N−TiO_2−cotton shows absorption in the visible light region, which is attributed to the presence of N−TiO_2 on the surface of cotton, which has narrow band gap and capability of visible light absorption (see Figure S6 in the Supporting Information. Moreover, AgI−N−TiO_2−cotton owns strong absorption in visible light region, which should be attributed to the presence of visible-light sensitizer AgI particles, which has a strong and wide absorption band in the visible light region.[15,21] Meanwhile, the band gap of AgI can be calculated by eq 1.[22]

$$\alpha h\nu = A(h\nu - E_g)^{n/2} \quad (1)$$

where α, ν, E_g, and A are absorption coefficient, light frequency, band gap, and a constant, respectively. Among them, n is determined by the type of optical transition of a semiconductor (i.e., n = 1 for direct transition and n = 4 for indirect transition). As AgI only exhibits the characteristic of direct band transition,[23] the values of n is 1. Therefore, the band gap energy of AgI is determined from a plot of $(\alpha h\nu)^2$ versus energy $(h\nu)$ (Figure 3) and found to be 2.86 eV, which is in accordance with the band gap of AgI particles previously reported.[24] At the same time, it is also inferred that no Ag nanoparticles are dispersed on the AgI−N−TiO_2−cotton, because there is no absorption above 450 nm (Figure 3), and the surface plasmon resonance (SPR) effect of silver should generate a broad absorption ranging from 400 to 800 nm.[25,26]

The nature of the surface species of as-prepared composite is studied by XPS surface probe technique, and the chemical states of nitrogen, silver and iodine on the surfaces of AgI−N−TiO_2-cotton were obtained by analyzing its XPS results. In our experiment, two N 1s peaks are found at 396 eV and around 400 eV (see Figure S7 in the Supporting Information. The

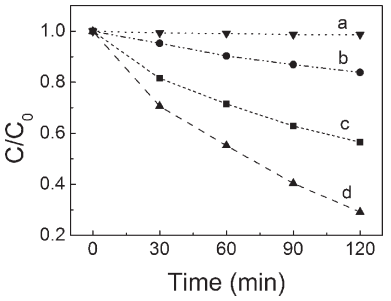

Figure 5. Photocatalytic activities of (a) cotton, (b) TiO_2−cotton, (c) N−TiO_2−cotton, and (d) AgI−N−TiO_2−cotton.

binding energy at 396 eV indicates that Ti−N binding is actually formed in the lattice of the titania crystal.[27,28] And the peak around 400 eV should be attributed to the N atoms existing in lattice space of TiO_2 nanoparticles.[29,30] From the XPS results (Figure 4), the binding energies of Ag $3d_{5/2}$ is 367 eV, which indicates that Ag is in the form of Ag^+ and no Ag^0 was formed.[14,16,21] The binding energies of I $3d_{5/2}$ is 618.4 eV, which indicates that I is present in the form of I^- assigned to AgI.[21] And there is no the existence of I_2, because the binding energies of I $3d_{5/2}$ in the form of I_2 is above 620 eV.[31,32] In addition, corresponding to result of XPS, the atomic ratio of silver and iodine on the surface of AgI−N−TiO_2−cotton was 1:1 approximately. According to the XRD, DRS and XPS patterns of the AgI−N−TiO_2−cotton fabrics, the following conclusion can be deduced that Ag^0 and I_2 have not been generated in the process of AgI loading.

Figure 5 shows the dependence of photocatalytic degradation of methyl orange (MO) under visible light irradiation on cotton, TiO_2−cotton, N−TiO_2−cotton and AgI−N−TiO_2−cotton. The photocatalytic degradation of MO under visible irradiation is not observed in the presence of the pristine cotton alone (Figure 5a) and the photocatalytic degradation of MO over TiO_2−cotton is very weak (Figure 5b). However, the photocatalytic activity of N−TiO_2−cotton was greatly enhanced and the MO removal over N−TiO_2−cotton reached 43% after two hours irradiation, which should be attributed to the existence of N−TiO_2. Nitrogen doping would result in narrowing the banding energy of TiO_2, and improving optical absorption performance of TiO_2, therefore N−TiO_2 can be excited under visible light irradiation.[11] Excitingly, the photocatalytic activity of AgI−N−TiO_2−cotton was greatly enhanced and the MO removal over AgI−N−TiO_2−cotton reached 71% after 2 h irradiation. The outstanding visible-light-induced photocatalytic activity of AgI−N−TiO_2−cotton should be attributed to the synergistic effect of N−TiO_2 and AgI. AgI also can introduce the visible-light-induced activity. Hu et al. reported that the photocatalyst AgI/P25 can be efficiently excited by visible light to create electron−hole pairs and form reactive oxygen species of •OH and O_2•$^-$ radical,[14] which have strong oxidizing ability to decompose almost all organic pollutants.[33,34] It is well-known that photocatalytic oxidation of organic pollutants follows first-order kinetics. The apparent rate constant (k) has been chosen as the basic kinetic parameter for the different photocatalysts, which was fitted by the eq 2

$$\ln(C/C_0) = -kt \quad (2)$$

where k is apparent rate constant, C is the solution-phase concentration of organic pollutant (in this case, MO), and C_0

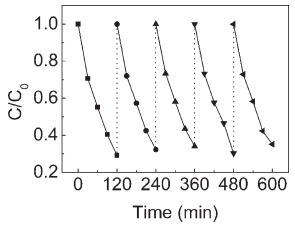

Figure 6. Photocatalytic activities of AgI−N−TiO_2−cotton upon repeated MO adsorption−illumination cycles.

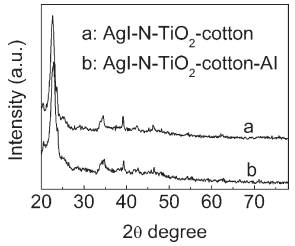

Figure 7. XRD spectra of AgI−N−TiO_2−cotton (a) before and (b) after irradiation.

Table 1. Absolute Electronegativity, Estimated Band Gap, Energy Levels of Calculated Conduction Band Edge, and Valence Band at the Point of Zero Charge for AgI and TiO_2, Energy Levels of Conduction Band Edge, and Valence Band of N-TiO_2

smicondutor oxides	absolute electronegativity (X)	estimated energy band gap (eV)	calculated conduction band edge (eV)	calculated valence band edge(eV)
AgI	5.48	2.86	−0.45	2.41
TiO_2	5.84	3.2	−0.26	2.94
N-TiO_2		2.93	−0.26	2.67

is the initial concentration of MO . The apparent rate constants of MO over TiO_2−cotton, N−TiO_2−cotton and AgI−N−TiO_2−cotton are 0.00153, 0.00506, and 0.01021 min^{-1}, respectively. The photocatalytic efficiency of AgI−N−TiO_2−cotton under visible-light irradiation is estimated to be about 6.67 and 2.02 times higher than that over TiO_2−cotton and N−TiO_2−cotton, respectively.

To evaluate the stability and reusability of the sample, we also performed a recyclability test involving repeated photodegradation of MO over AgI−N−TiO_2−cotton. As shown in Figure 6, after five cycles of the photodegradation of MO, AgI−N−TiO_2−cotton did not exhibit any significant loss of activity, indicating its good stability for repeated photocatalysis. Meanwhile, comparing of the XRD patterns of AgI−N−TiO_2−cotton before and after three times of cycle experiment (Figure 7), the diffraction peaks of AgI have no visible change. From the photocatalytic performances and the XRD patterns, it is confirmed that AgI/N−TiO_2−cotton could be used as stable and efficient visible-light-induced self-cleaning materials

The enhancement and the stability of photocatalytic activity of AgI−N−TiO_2−cotton under visible light irradiation should be attributed to the configuration of the AgI/N−TiO_2 composites.

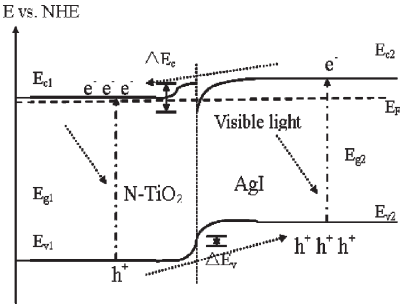

Figure 8. Energy band diagram of the AgI/N−TiO_2 heterojunction and the possible migration processes of photogenerated carriers under visible-light irradiation.

The band edge positions of AgI and TiO_2 can be predicted theoretically from the absolute (or Mulliken) electronegativity.[35−38] The conduction band edge of a semiconductor at the point of zero charge (pH_{zpc}) can be estimated by eq 3

$$E_{CB}{}^{0} = X - E^{c} - 1/2E_{g} \quad (3)$$

where X is the absolute electronegativity of the semiconductor, expressed as the geometric mean of the absolute electronegativity of the constituent atoms, which is defined as the arithmetic mean of the atomic electron affinity and the first ionization energy; E^c is the energy of free electrons on the hydrogen scale (4.5 eV); and E_g is the band gap of the semiconductor. The band edge positions of AgI and TiO_2 estimated by above equation are shown in Table 1. Meanwhile, we know that nitrogen doping does not change the conduction band position of TiO_2 but the valence band position of TiO_2, because the conduction band of N-doped TiO_2 consist mainly of 3d orbitals of the Ti atom.[39] Thus, the conduction band and valence band positions of N−TiO_2 can be estimated using the data of TiO_2, as shown in Table 1. According to the result (Table 1), the conduction band position of AgI is more cathodic than N−TiO_2, and the valence band position of N−TiO_2 is more anodic than AgI. In addition, AgI behaves as an n-type semiconductor[40] and N−TiO_2 also behaves as an n-type semiconductor,[41] as a result, the contact between N−TiO_2 and AgI fabricates an n-n heterojunction. The energy-band diagrams of AgI/N−TiO_2 composite photocatalysts are shown in Figure 8. In Figure 8, the subscripts 1 and 2 refer to N−TiO_2 and AgI; E_g is the band gap; E_F is the Fermi level; E_c and E_v are conduction and valence band edge, respectively; ΔE_c is the conduction band edge discontinuity (conduction-band offset), $\Delta E_c = x_1 - x_2$, x is the electron affinity of semiconductor; ΔE_v is the valence band edge discontinuity, $\Delta E_v = (E_{g2} - E_{g1}) - (x_1 - x_2)$.[42] Under visible-light irradiation, both N−TiO_2 and AgI can be excited to produce electron−hole pairs. According to the band edge position, holes move to AgI side, and electrons migrate to the N−TiO_2 side. Thereby, the chance of electron−hole recombination is reduced. This leads to an enhanced photocatalytic activity in the photooxidation of methyl orange. At the same time, the AgI/N−TiO_2 composites enable AgI to be more stable under irradiation because of the lower electrons concentration in the conduction band of AgI.

CONCLUSIONS

AgI−N−TiO_2−cotton has been successfully fabricated by a facile and effective method. The prepared AgI−N−TiO_2−cotton displays enhanced visible light absorption, and the photocatalytic activity against methyl orange is greatly improved in comparison with TiO_2−cotton. The dramatic enhancement in

the visible light photocatalytic performance of the AgI−N−TiO_2−cotton should be attributed to the synergistic effect of AgI and N−TiO_2. On the one hand, because of narrow band gap, AgI and N−TiO_2 all introduce photocatalytic activity under visible light irradiation. On the other hand, the band edge positions of AgI and N-TiO_2 facilitate the transfer of the photoinduced carriers. Meanwhile, the experiments prove that AgI is stable under visible l−ght irradiation, indicating AgI−N−TiO_2−cotton can be used as efficient visible-light-induced self-cleaning materials.

■ ASSOCIATED CONTENT

Supporting Information. Supplementary data include the following contexts: TEM micrograph and SAED pattern of N−TiO_2, the EDX spectrum and map of AgI−N−TiO_2−cotton, the contrast of XRD patterns between cotton and N−TiO_2, XRD of N−TiO_2, UV−vis absorption spectra of N−TiO_2 and N1s X-ray photoelectron spectra. This material is available free of charge via the Internet at http://pubs.acs.org.

■ AUTHOR INFORMATION

Corresponding Author

*E-mail: wdy001815@126.com (D.W.); long_mc@sjtu.edu.cn (M.L.).

■ ACKNOWLEDGMENT

This project was funded by State Key Laboratory for Modification of Chemical Fibers and Polymer Materials, Dong Hua University (LK0907) and by National Natural Science Foundation of China (20907031).

■ REFERENCES

(1) Sanchez, M.; Rivero, M. J.; Ortiz, I. *Appl. Catal., B* **2011**, *101*, 515–521.
(2) Lü, X. J.; Ding, S. J.; Xie, Y.; Huang, F. Q. *Eur. J. Inorg. Chem.* **2011**, *2011*, 2879–2883.
(3) Shan, A. Y.; Ghazi, T. I. M.; Rashid, S. A. *Appl. Catal., A* **2010**, *389*, 1–8.
(4) Li, Y. J.; Chen, W.; Li, L. Y.; Ma, Y. *Sci. China Chem.* **2011**, *54*, 497–505.
(5) Daoud, W. A.; Leung, S. K.; Tung, W. S.; Xin, J. H.; Cheuk, K.; Qi, K. *Chem. Mater.* **2008**, *20*, 1242–1244.
(6) Wu, D. Y.; Long, M. C.; Zhou, J. Y.; Cai, W. M.; Zhu, X. H.; Chen, C.; Wu, Y. H. *Surf. Coat. Technol.* **2009**, *203*, 3728–3733.
(7) Yaghoubi, H.; Taghavinia, N.; Alamdari, E. K. *Surf. Coat. Technol.* **2010**, *204*, 1562–1568.
(8) Uddin, M. J.; Cesano, F.; Bonino, F.; Bordiga, S.; Spoto, G.; Scarano, D.; Zecchina, A. *J. Photochem. Photobiol., A* **2007**, *189*, 286–294.
(9) Uddin, M. J.; Cesano, F.; Scarano, D.; Bonino, F.; Agostini, G.; Spoto, G.; Bordiga, S.; Zecchina, A. *J. Photochem. Photobiol., A* **2008**, *199*, 64–72.
(10) Uddin, M. J.; Cesano, F.; Bertarione, S.; Bonino, F.; Bordiga, S.; Scarano, D.; Zecchina, A. *J. Photochem. Photobiol., A* **2008**, *196*, 165–173.
(11) Asahi, R.; Morikawa, T.; Ohwaki, T.; Aoki, K.; Taga, Y. *Science* **2001**, *293*, 269–271.
(12) Horikoshi, S.; Minatodani, Y.; Sakai, H.; Abe, M.; Serpone, N. *J. Photochem. Photobiol., A* **2011**, *217*, 191–200.
(13) Wu, D. Y.; Long, M. C.; Cai, W. M.; Chen, C.; Wu, Y. H. *J. Alloys Compd.* **2010**, *502*, 289–294.
(14) Hu, C.; Hu, X. X.; Wang, L. S.; Qu, J. H.; Wang, A. M. *Environ. Sci. Technol.* **2006**, *40*, 7903–7907.
(15) Hu, C.; Guo, J.; Qu, J. H.; Hu, X. X. *Langmuir* **2007**, *23*, 4982–4987.
(16) Cheng, H. F.; Huang, B. B.; Dai, Y.; Qin, X. Y.; Zhang, X. Y. *Langmuir* **2010**, *26*, 6618–6624.
(17) Birks, L. S.; Friedman, H. *J. Appl. Phys.* **1946**, *17*, 687–692.
(18) He, H. P.; Wang, Y. X.; Chen, H. W. *Solid State Ionics* **2004**, *175*, 651–654.
(19) Bernard, Ng, C. H.; Fan, W. Y. *J. Phys. Chem. C* **2007**, *111*, 2953–8.
(20) Nagai, M.; Nishino, T. *Solid State Ionics* **1999**, *117*, 317–321.
(21) Li, Y. Z.; Zhang, H.; Guo, Z. M.; Han, J. J.; Zhao, X. J.; Zhao, Q. N.; Kim, S. J. *Langmuir* **2008**, *24*, 8351–8357.
(22) Butler, M. A. *J. Appl. Phys.* **1977**, *48*, 1914–1920.
(23) Victora, R. H. *Phys. Rev. B* **1997**, *56*, 4417–4421.
(24) Chen, S. H.; Ida, T.; Kimura, K. *J. Phys. Chem. B* **1998**, *102*, 6169–6176.
(25) Wu, T. S.; Wang, K. X.; Li, G. D.; Sun, S. Y.; Sun, J.; Chen, J. S. *ACS Appl. Mater. Interfaces* **2010**, *2*, 544–550.
(26) Wang, J. Y.; Zhao, H. T.; Liu, X. R.; Li, X. D.; Xu, P.; Han, X. J. *Catal. Commun.* **2009**, *10*, 1052–1056.
(27) Xing, M. Y.; Zhang, J. L.; Chen, F. *Appl. Catal., B* **2009**, *89*, 563–569.
(28) Cantau, C.; Pigot, T.; Dupin, J. C.; Lacombe, S. *J. Photochem. Photobiol., A* **2011**, *216*, 201–208.
(29) Di Valentin, C.; Pacchioni, G.; Selloni, A.; Livraghi, S.; Giamello, E. *J. Phys. Chem. B* **2005**, *109*, 11414–11419.
(30) Yu, A. M.; Wu, G. J.; Zhang, F. X.; Yang, Y. L.; Guan, N. J. *Catal. Lett.* **2009**, *129*, 507–512.
(31) Salaneck, W. R.; Thomas, H. R.; Bigelow, R. W.; Duke, C. B.; Plummer, E. W.; Heeger, A. J.; Macdiarmid, A. G. *J. Chem. Phys.* **1980**, *72*, 3674–3678.
(32) Polzonetti, G.; Faruffini, V.; Furlani, A.; Russo, M. V. *Synth. Met.* **1989**, *29*, 495–499.
(33) Lawless, D.; Serpone, N.; Meisel, D. *J. Phys. Chem.* **1991**, *95*, 5166–5170.
(34) Noguchi, T.; Fujishima, A. *Environ. Sci. Technol.* **1998**, *32*, 3831–3833.
(35) Kim, Y.; Atherton, S. J.; Brigham, E. S.; Mallouk, T. E. *J. Phys. Chem.* **1993**, *97*, 11802–11810.
(36) Butler, M. A.; Ginley, D. S. *J. Electrochem. Soc.* **1978**, *125*, 228–232.
(37) Xu, Y.; Schoonen, M. A. A. *Am. Mineral.* **2000**, *85*, 543–556.
(38) Long, M.; Cai, W. M.; Cai, J.; Zhou, B. X.; Chai, X. Y.; Wu, Y. H. *J. Phys. Chem. B* **2006**, *110*, 20211–20216.
(39) Long, M. C.; Cai, W. M.; Wang, Z. P.; Liu, G. Z. *Chem. Phys. Lett.* **2006**, *420*, 71–76.
(40) Patnaik, J. R. G.; Sunandana, C. S. *J. Phys. Chem. Solids* **1998**, *59*, 1059–1069.
(41) Wang, Y. Q. *Chin. J. Inorg. Chem.* **2006**, *22*, 1349–1353.
(42) Liu, S.; Wu, J. T.; Liu, X. P.; Jiang, R. Y. *J. Photochem. Photobiol., A* **2010**, *332*, 84–92.